A HYBRID AGGRESSIVE SPACE MAPPING
ALGORITHM FOR EM OPTIMIZATION

M.H. Bakr, J.W. Bandler, K. Madsen and N. Georgieva

SOS-98-22-R

August 1998

A HYBRID AGGRESSIVE SPACE MAPPING
ALGORITHM FOR EM OPTIMIZATION

M.H. Bakr, J.W. Bandler, K. Madsen and N. Georgieva

Simulation Optimization Systems Research Laboratory
and Department of Electrical and Computer Engineering
McMaster University, Hamilton, Canada L8S 4L7

Abstract

In this work we present a novel algorithm for the aggressive space mapping of microwave circuits. This algorithm exploits a hybrid approach between the trust region aggressive space mapping (TRASM) and direct optimization. Space mapping is very efficient in terms of the needed fine model simulations. The final space-mapped design may not be the optimal fine model design. Severe misalignment between the coarse model and the fine model is likely to cause space mapping not to work. To overcome this a hybrid algorithm that connects space mapping and direct optimization is presented. This connection is based on a novel theorem that enables a smooth switching from space mapping to direct optimization and vice versa. We tested the new algorithm using a number of examples and the results are encouraging.

I. INTRODUCTION

In this work we present a novel hybrid space mapping algorithm. Space mapping is an interesting concept. It aims at directing most of the optimization computational effort towards a fast coarse model while maintaining the accuracy of a fine model. The computational effort needed is much smaller than that needed for direct optimization.

In the first introduced space mapping algorithm [1] a set of fine model points is needed to establish the initial mapping between the two spaces. In each other iteration, only one fine model point is required to make a new iterate and update the mapping. The aggressive space mapping (ASM) technique [2] was later introduced to eliminate this overhead. No initial set of points is needed and only one fine model simulation is needed for every iteration.

The parameter extraction step is a crucial procedure in the space mapping technique [3]. In this step a coarse model point whose response matches a given fine model response is obtained. This procedure is essentially an optimization procedure. The nonuniqueness of the extracted parameters may lead to the divergence or oscillation of the iterations [3].

To overcome this problem the TRASM algorithm was introduced [4]. This algorithm integrates a trust region methodology [5] with the aggressive space mapping. Also, the algorithm utilizes a recursive multi-point parameter extraction with the aim of improving the uniqueness of the extraction step. The available information about the mapping between the two spaces is also utilized in this step.

The design obtained by space mapping in most cases is an optimal or near optimal design. However, the optimality of the final design can not be guaranteed. This is because the final space-mapped response matches the optimal coarse model response which may be different from the optimal fine model response obtained by direct optimization.

Space mapping also assumes that the coarse model is not severely different from the fine model. If the coarse model is not good enough space mapping is unlikely to converge.

In this work we present a novel algorithm that aims at solving these problems. The algorithm is a hybrid one between space mapping and direct optimization. The final design obtained by this algorithm is the optimal fine model design. The algorithm is based on a novel theorem that enables switching between space mapping and direct optimization in a smooth way. The algorithm defaults to direct optimization if space mapping fails. It defaults to space mapping if space mapping is converging smoothly. The algorithm also utilizes all the information available from space mapping in direct optimization and vice versa.

We start by giving a brief review of space mapping in Section II. In Section III we discuss the motivation behind the new algorithm. A novel theorem that enables switching between space mapping and direct optimization is presented in Section IV. The new algorithm is explained in Section V. The algorithm was successfully applied to a number of examples. The obtained results are given in Section VI. Finally, the conclusions are given in Section VII.

II. SPACE MAPPING: A BRIEF REVIEW

It is assumed that the circuit under consideration can be simulated using two models: a fine model and a coarse model. The fine model is accurate but is computationally intensive. This model can, for example, be a finite element model. We refer to the vector of parameters of this model as x_{em}. The coarse model is a fast model but it is less accurate than the fine model. This model can be a circuit-theoretic empirical model. The vector of parameters of this model is referred to as x_{os}.

The first step of the technique is to obtain the optimal design of the coarse model x_{os}^*. The technique aims at establishing a mapping P between the two spaces [2]

$$x_{os} = P(x_{em}) \tag{1}$$

such that

$$\left\| R_{em}(x_{em}) - R_{os}(x_{os}) \right\| \leq e \tag{2}$$

where R_{em} is the vector of fine model responses, R_{os} is the vector of coarse mode responses and $\| \ \|$ is a suitable norm. The error function

$$f = P(x_{em}) - x_{os}^*$$ (3)

is first defined. The final fine model design is obtained and the mapping is established if a solution for the system of nonlinear equations

$$f(x_{em}) = 0$$ (4)

is found.

Let $x_{em}^{(i)}$ be the ith iterate in the solution of (4). In the ASM technique, the next iterate $x_{em}^{(i+1)}$ is found by a quasi-Newton iteration

$$x_{em}^{(i+1)} = x_{em}^{(i)} + h^{(i)}$$ (5)

where $h^{(i)}$ is obtained from

$$B^{(i)} h^{(i)} = -f(x_{em}^{(i)})$$ (6)

and $B^{(i)}$ is an approximation to the Jacobian of the vector f with respect to x_{em} at the ith iteration. The matrix B is updated at each iteration using Broyden's update [6].

It is clear from (1)-(3) that the vector function f is obtained by evaluating $P(x_{em})$. This can be achieved through the process of parameter extraction. This process involves solving another optimization problem. This optimization problem may have more than one minimum and this may lead to the divergence of the ASM technique.

To overcome the nonuniqueness of the parameter extraction problem, the TRASM algorithm [4] was introduced. At the ith iteration, the residual vector $f^{(i)} = P(x_{em}^{(i)}) - x_{os}^*$ defines the difference between the vector of extracted coarse model parameters $x_{os}^{(i)} = P(x_{em}^{(i)})$ and the optimal coarse model design. The mapping between the two models is established if this residual vector is driven to zero. It

follows that the value $\left\|\boldsymbol{f}^{(i)}\right\|$ can serve as a measure of the misalignment between the two spaces in the ith iteration. The step taken in the ith iteration is obtained from

$$(\boldsymbol{B}^{(i)T}\boldsymbol{B}^{(i)} + l\,\boldsymbol{I})\boldsymbol{h}^{(i)} = -\boldsymbol{B}^{(i)T}\boldsymbol{f}^{(i)} \tag{7}$$

where $\boldsymbol{B}^{(i)}$ is an approximation to the Jacobian of the coarse model parameters with respect to the fine model parameters at the ith iteration. The parameter l is selected such that the step obtained satisfies $\left\|\boldsymbol{h}^{(i)}\right\| \le d$ where d is the size of the trust region. This is done by utilizing the iterative algorithm suggested in [5]. Solving (7) corresponds to minimizing $\left\|\boldsymbol{f}^{(i)} + \boldsymbol{B}^{(i)}\boldsymbol{h}^{(i)}\right\|_2^2$ subject to $\left\|\boldsymbol{h}^{(i)}\right\|_2 \le d$.

Single-point parameter extraction is then applied to the new fine model point. This point is accepted if it satisfies a certain success criterion with respect to the reduction in the ℓ_2 norm of the vector $\boldsymbol{f}$. Otherwise, the uniqueness of the parameter extraction process is suspect. To improve the uniqueness of the step, a future point is generated and is added to the set of fine model points used for the multi-point parameter extraction. This is repeated until either the extracted coarse model parameters approach a limit or the number of accumulated fine model points reaches $n+1$. If the vector of extracted parameters approaches a limit without satisfying the success criterion we trust the parameter extraction process. In this case, the failure of the step is attributed to the large trust region size. The trust region size is then shrunk and (7) is resolved. If the number of accumulated fine model points reaches $n+1$ sufficient information is available to obtain an estimate for the Jacobian of the fine model responses with respect to the fine model parameters. This Jacobian matrix is used to predict an alternative step to that predicted by (7).

III. LIMITATIONS OF SPACE MAPPING

The ASM technique and the TRASM algorithm are extremely efficient algorithms. The number of fine model simulations needed to obtain the space-mapped design is of the order of the problem

dimensionality. However, it should be noted that both algorithms depend on the existence of a coarse model that is fast and has enough accuracy.

If the coarse model is a bad one (i.e., extremely different from the fine model) space mapping might not work. To illustrate this we consider the Rosenbrock function [7]. We form an artificial problem in which the coarse model is given by

$$R_{os} = 100\,(x_2 - x_1^2)^2 + (1 - x_1)^2 \tag{8}$$

The fine model is another Rosenbrock function but with the parameters x_1 and x_2 shifted by two shifts $\boldsymbol{a}_1$ and $\boldsymbol{a}_2$, respectively. It follows that the fine model is given by

$$R_f = 100\,((x_2 + \boldsymbol{a}_2) - (x_1 + \boldsymbol{a}_1)^2)^2 + (1 - (x_1 + \boldsymbol{a}_1))^2 \tag{9}$$

The optimal solution of the coarse model is $\boldsymbol{x}_{os}^* = [1.0 \quad 1.0]^T$ while the optimal fine model solution is given by $\boldsymbol{x}_f^* = [(1 - \boldsymbol{a}_1) \quad (1 - \boldsymbol{a}_2)]^T$. The misalignment between the two models is given by the two shifts $\boldsymbol{a}_1$ and $\boldsymbol{a}_2$. First, we consider the case when $\boldsymbol{a}_1 = -0.1$ and $\boldsymbol{a}_2 = -0.1$. The coarse model in this case is a good one. The contours of $\|\boldsymbol{f}\|_2^2$ are shown in Fig. 1. These contours were obtained analytically using two-point parameter extraction. It is clear that $\|\boldsymbol{f}\|_2^2$ has a single minimum which is the minimum that would be obtained if direct optimization is applied to the fine model. Starting from the point $\boldsymbol{x}_{os}^*$ the TRASM algorithm is guaranteed to converge to the optimal fine model design. The corresponding contours of R_f are shown in Fig. 2. Next, we increase the misalignment between the two models by making $\boldsymbol{a}_1 = -0.9$ and $\boldsymbol{a}_2 = -0.9$. The contours of $\|\boldsymbol{f}\|_2^2$ are shown in Fig. 3. It is clear that $\|\boldsymbol{f}\|_2^2$ still has a minimum at the optimal fine model design ($[1.9 \quad 1.9]^T$). However, other minima of $\|\boldsymbol{f}\|_2^2$ exist. It follows that applying the TRASM algorithm starting from the point $\boldsymbol{x}_{os}^*$ may not converge to the optimal fine model solution. The corresponding contours of R_f are shown in Fig. 4.

Finally, we make the misalignment between the two models severe by assigning $a_1 = -1.5$ and $a_2 = -1.5$. For this case, the contours of $\|f\|_2^2$ are shown in Fig. 5. In this case, the TRASM algorithm will certainly converge to a minimum other than the optimal fine model solution. The corresponding contours of R_f are shown in Fig. 6.

This example shows that space mapping may fail if the coarse model is severely different from the fine model. One other thing that should be noted is that in many problems the optimal coarse model response is not equal to the optimal fine model response. For example, consider the coarse model

$$R_{os} = 100\,(x_2 - x_1^2)^2 + (1 - x_1)^2 + e \tag{10}$$

where $e > 0$. Assume also that the fine model is given by

$$R_{em} = 100\,(x_2 - x_1^2)^2 + (1 - x_1)^2 \tag{11}$$

It is clear from (10) that the optimal coarse model response is e while the optimal fine model response is zero. It follows that in such a case, even if space mapping converges, the space-mapped fine model design may not be the optimal fine model design.

The discussed limitations of space mapping suggest that a hybrid technique be used. This technique exploits the efficiency of space mapping and defaults to direct optimization when space mapping fails. We discuss the proposed hybrid algorithm in Section V. But before introducing the new algorithm we present a novel theorem relating space mapping to direct optimization.

IV. SPACE MAPPING AND DIRECT OPTIMIZATION

In this section we introduce a very interesting theorem that allows for smooth switching between direct optimization and space mapping.

Lemma 1.

Assume that the two points x_{os} and x_{em} are two corresponding points in the coarse model space and fine model space, respectively and that the mapping between the two spaces at these two

corresponding points is given by the matrix $\boldsymbol{B}$. It follows that the Jacobian of the fine model responses at the point $\boldsymbol{x}_{em}$ is given by

$$\boldsymbol{J}_{em} = \boldsymbol{J}_{os}\boldsymbol{B} \tag{12}$$

where $\boldsymbol{J}_{os}$ is the Jacobian of the coarse model responses at the point $\boldsymbol{x}_{os}$.

Proof

As the points $\boldsymbol{x}_{em}$ and $\boldsymbol{x}_{os}$ correspond to each other, it follows that their corresponding responses match, i.e.,

$$\boldsymbol{R}_{em}(\boldsymbol{x}_{em}) = \boldsymbol{R}_{os}(\boldsymbol{x}_{os}) \tag{13}$$

Now define a new fine model point $\boldsymbol{x}_n = \boldsymbol{x}_{em} + \Delta\boldsymbol{x}_{em}$ where $\Delta\boldsymbol{x}_{em}$ is a small perturbation. The response at this new point is perturbed from the response at the point $\boldsymbol{x}_{em}$ by

$$\Delta\boldsymbol{R} = \boldsymbol{J}_{em}\Delta\boldsymbol{x}_{em} \tag{14}$$

The point $\boldsymbol{x}_n$ corresponds to a coarse model point $\boldsymbol{x}_{os} + \Delta\boldsymbol{x}_{os}$ which satisfies

$$\Delta\boldsymbol{R} = \boldsymbol{J}_{em}\Delta\boldsymbol{x}_{em} = \boldsymbol{J}_{os}\Delta\boldsymbol{x}_{os} \tag{15}$$

Also, the two perturbations $\Delta\boldsymbol{x}_{em}$ and $\Delta\boldsymbol{x}_{os}$ are related by

$$\boldsymbol{B}\Delta\boldsymbol{x}_{em} = \Delta\boldsymbol{x}_{os} \tag{16}$$

multiplying both sides of (16) by $\boldsymbol{J}_{os}$ we get

$$\boldsymbol{J}_{os}\boldsymbol{B}\Delta\boldsymbol{x}_{em} = \boldsymbol{J}_{os}\Delta\boldsymbol{x}_{os} \tag{17}$$

Comparing (17) with (15) we conclude that

$$\boldsymbol{J}_{em} = \boldsymbol{J}_{os}\boldsymbol{B} \tag{18}$$

Relation (18) is interesting. It shows that by having the matrix $\boldsymbol{B}$ and the coarse model Jacobian $\boldsymbol{J}_{os}$ we are able to obtain a good estimate of the Jacobian of the fine model responses without any further fine model simulations. It follows that when the space mapping is not converging smoothly we can switch to direct optimization and supply it with available first order derivatives given by (18).

Another interesting relationship which can be easily obtained from (18) is

$$B = \left(J_{os}^T J_{os} \right)^{-1} J_{os}^T J_{em} \tag{19}$$

Relation (19) assumes that the matrix J_{os} is a full rank matrix and $m > n$, where n is the number of parameters and m is the number of responses . It shows that the matrix B can be obtained by multiplying the Jacobian of the fine model responses with the pseudoinverse of the matrix J_{os} . A similar formula can be obtained using SVD if the matrix J_{os} is not full rank.

The relation (19) is used to switch back from direct optimization to space mapping. At the end of the iterations carried out using direct optimization the Jacobian of the fine model responses is available. Parameter extraction can be applied at this point to get the corresponding coarse model point. The Jacobian of the coarse model responses J_{os} at this coarse model point can be easily obtained. Relation (19) can then be used to regenerate the matrix B and the space mapping algorithm can resume normally. Fig. 7 illustrates the connection between space mapping and direct optimization.

To illustrate the theorem we consider the following one-dimensional example. The fine model is given by $R_f = sin(x)$ for $0 \le x \le \pi$ and the coarse model is given by $R_{os} = x / p$ for $0 \le x \le \pi$ as shown in Fig. 8. Clearly, the two subset $0 \le x \le \pi/2$ and $\pi/2 \le x \le \pi$ in the fine model space can be mapped to the subset $0 \le x \le \pi$ in the coarse model space. Thus we have two different mappings for these two different subsets of the fine model space. We first consider the point $x_f = \pi/4$ which belongs to the first set of the fine model space. The fine model response at this point is $R_f = 0.707$. To get the coarse model point that matches the same response parameter extraction is applied. The corresponding coarse model point is found to be $x_{os} = 2.2211$. To estimate the matrix B (a scalar in this case) we evaluate the fine model response at the point $x_f = \pi/4 + 0.05$ and parameter extraction is then applied to get the corresponding coarse model point which is found to be $x_{os} = 2.3296$. It follows that the matrix B can be approximated by

$$B \approx \frac{\Delta x_{os}}{\Delta x_f} = \frac{2.3296 - 2.2211}{0.05} = 2.17 \tag{20}$$

The coarse model has a linear equation and thus constant derivative. It follows that the derivative of the coarse model at the point x_{os}=2.2211 is $\boldsymbol{J}_{os}$ =1/π. From (18) the derivative of the fine model at the point x_f =[π/4] is

$$\boldsymbol{J}_{em} = \frac{2.17}{\boldsymbol{P}} = 0.6907 \tag{21}$$

Which is almost identical to the actual value of the derivative of the fine model (0.707). Using smaller perturbation than 0.05 would result in a better approximation to the matrix $\boldsymbol{B}$ and thus to a better approximation to the Jacobian matrix $\boldsymbol{J}_{em}$.

The same steps applied to the first set of fine model points is repeated for the second set of points. We selected the point $x_f = 7\pi/8$. The corresponding point in the coarse model space is found to be x_{os}=1.202235. A neighboring fine model point $x_f = 7\pi/8+0.02$ is selected. It is found that the corresponding coarse model point is x_{os}=1.14394. It follows that the matrix $\boldsymbol{B}$ can be approximated by

$$\boldsymbol{B} \approx \frac{\Delta x_{os}}{\Delta x_f} = \frac{1.14394 - 1.202235}{0.02} = -2.9142 \tag{22}$$

It follows that the Jacobian of the fine model responses is given by

$$\boldsymbol{J}_{em} = \frac{-2.9142}{\boldsymbol{P}} = -0.9276 \tag{23}$$

The exact value for the Jacobian of the fine model response is $\boldsymbol{J}_{em}$=−0.9238 which is almost identical to the one estimated in (23).

This one dimensional example shows clearly that the accuracy of the fine model Jacobian estimated using (18) depends on the accuracy of the matrix $\boldsymbol{B}$.

To further illustrate the theorem we discuss a two-dimensional problem. The fine model is given by

$$R_f = (0.9x_1+0.1x_2)^2 + (0.1x_1+0.9x_2)^2 \tag{24}$$

and the coarse model is given by

$$R_{os} = x_1^2 + x_2^2 \tag{25}$$

We consider the fine model point $x_f = [2.0 \quad 1.0]^T$. The fine model response at this point is $R_f = 4.82$

The corresponding coarse model point is obtained by applying multi-point parameter extraction [3] and is found to be $x_{os} = [1.84064 \quad 1.19404]^T$. Five fine model points were utilized in the multi-point extraction to ensure the uniqueness of the extraction phase. The Jacobian of the coarse model at this extracted point is given by

$$J_{os} = [3.68128 \quad 2.38808] \tag{26}$$

Using (24) and (25) we see that the mapping is given by

$$B = \begin{bmatrix} 0.9 & 0.1 \\ 0.1 & 0.9 \end{bmatrix} \tag{27}$$

Using (18) the Jacobian of the fine model at the point $x_f = [2.0 \quad 1.0]^T$ is approximated by

$$J_{em} = [3.68128 \quad 2.38808] \begin{bmatrix} 0.9 & 0.1 \\ 0.1 & 0.9 \end{bmatrix} = [3.55196 \quad 2.5174] \tag{28}$$

The exact fine model Jacobian is $J_{em} = [3.64 \quad 2.36]$. The difference between the exact Jacobian and the estimated one is attributed mainly to the accuracy of the multi-point parameter extraction. The exact solution for the parameter extraction is $[1.90 \quad 1.10]^T$. The Jacobian of the coarse model at the exact solution of parameter extraction is

$$J_{os} = [3.8 \quad 2.2] \tag{29}$$

The corresponding Jacobian estimate for this case is given by

$$J_{em} = [3.8 \quad 2.2] \begin{bmatrix} 0.9 & 0.1 \\ 0.1 & 0.9 \end{bmatrix} = [3.64 \quad 2.36] \tag{30}$$

which is the exact Jacobian of the fine model.

The two discussed examples show clearly that the theorem can effectively obtain good approximate for the Jacobian of the fine model responses using the matrix B and the Jacobian of the

coarse model responses J_{os}. Also these examples show that the accuracy of the obtained estimate for the Jacobian of the fine model responses depends on the accuracy of the matrix B and on the accuracy of the parameter extraction problem.

V. THE NEW ALGORITHM

The new algorithm exploits the efficiency of space mapping when this is possible and defaults to direct optimization when space mapping fails to make any progress. The objective function of the TRASM algorithm is

$$\|f\|_2^2 = \|P(x_{em}) - x_{os}^*\|_2^2 \tag{31}$$

The objective function for direct optimization is

$$\|g\|_2^2 = \|R_{em}(x_{em}) - R_{os}(x_{os}^*)\|_2^2 \tag{32}$$

The main target of the hybrid algorithm is to minimize the objective function (32). In the ith iteration we assume the existence of a trusted extracted coarse model parameters $P(x_{em}^{(i)})$. The step taken in this iteration is given by (7) where $x_{em}^{(i+1)} = x_{em}^{(i)} + h^{(i)}$. Single-point parameter extraction is then applied at the point $x_{em}^{(i+1)}$ to get $f^{(i+1)} = P(x_{em}^{(i+1)}) - x_{os}^*$. We accept this point if it satisfies a certain success criteria with respect to the reductions in both objective functions (31) and (32). The matrix $B^{(i)}$ is then updated using Broyden's formula [6] and space mapping resumes. Otherwise, a switch to the phase (direct optimization) takes place.

There are two forms of failure of the space mapping iteration that may occur. The first form is that the success criterion of (32) is not satisfied which means that we have to reject the new point $x_{em}^{(i+1)}$. The Jacobian of the fine model responses at the point $x_{em}^{(i)}$ is then evaluated. This is done by first evaluating the Jacobian of the coarse model responses $J_{os}^{(i)}$ at the point $x_{os}^{(i)} = P(x_{em}^{(i)})$. The matrix $J_{em}^{(i)}$ is then evaluated using $J_{em}^{(i)} = J_{os}^{(i)} B^{(i)}$. Both $x_{em}^{(i)}$ and $J_{em}^{(i)}$ are then supplied to the second phase.

The second form of failure of space mapping which may occur is that the new point $x_{em}^{(i+1)}$ satisfies the success criterion of (32) but does not satisfy the success criterion of (31). In this case the point $x_{em}^{(i+1)}$ is better than the previous point $x_{em}^{(i)}$ and is accepted. As the vector of extracted parameters does not satisfy the success criterion of (31), the vector $f^{(i+1)}$ can not be trusted. In order to trust this vector, recursive multi-point parameter extraction is applied at the point $x_{em}^{(i+1)}$ until either it approaches a limiting value or the number of additional points used for multi-point parameter extraction reaches n. If $f^{(i+1)}$ approaches a limit that satisfies the success criterion of (31) space mapping resumes and the matrix B is updated. If $f^{(i+1)}$ approaches a limit that does not satisfy the success criterion of (31) the matrix $B^{(i+1)}$ is update using the Broyden's formula, the matrix $J_{os}^{(i+1)}$ at the point $x_{os}^{(i+1)}=P(x_{em}^{(i+1)})$ is evaluated and the matrix $J_{em}^{(i+1)}$ is then evaluated using $J_{em}^{(i+1)} = J_{os}^{(i+1)} B^{(i+1)}$. Otherwise, the matrix $J_{em}^{(i+1)}$ is approximated using the fine model points used for multi-point parameter extraction. In both cases, both the point $x_{em}^{(i+1)}$ and the matrix $J_{em}^{(i+1)}$ are supplied to the second phase.

The second phase utilizes the first order derivatives supplied by space mapping to carry out a number of successful iterations. By a successful iteration we mean an iteration that satisfies the success criterion of (32). At the end of each successful iteration parameter extraction is applied at the new iterate $x_{em}^{(k)}$ and is used to check whether the success criterion of (31) is satisfied. If it is satisfied the coarse model Jacobian matrix $J_{os}^{(k)}$ at the point $x_{os}^{(k)}=P(x_{em}^{(k)})$ is evaluated, the matrix B is reevaluated using $B = \left(J_{os}^{(k)T} J_{os}^{(k)} \right)^{-1} J_{os}^{(k)T} J_{em}^{(k)}$ and the algorithm switches back to phase 1. The superscript k is used as an index for the successful iterates of the direct optimization phase. If the success criterion of (31) is not satisfied phase 2 continues.

The objective function (32) aims at matching the fine model response to the optimal coarse model response but this does not ensure the optimality of the space-mapped solution if the optimal coarse model response is different from the optimal fine model response. This motivates the suggestion that if

13

the second phase has reached a point where no more improvement in the objective function (32) is possible, direct optimization solves the original design problem in the fine model space using a minimax optimizer [8]. The objective function of the minimax optimizer is

$$\max_k e_k \tag{33}$$

where

$$e_k = R_{em,k} - S_{u,k} \qquad \text{if } k \in K_u \tag{34}$$

$$e_k = S_{l,k} - R_{em,k} \qquad \text{if } k \in K_l \tag{35}$$

where $S_{u,k}$ is the kth upper constraint and $S_{l,k}$ is the kth lower constraint and the sets K_u and K_l are sets of indices for upper and lower constraints, respectively. The starting point for this minimax problem is the final design of the second phase obtained using the objective function (32). This part is mainly added to ensure the optimality of the obtained designs.

For any iteration $i \geq 0$, the two phases are given by the following steps.

Phase 1

Step 0   Given $x_{em}^{(i)}$, $f^{(i)}$, $B^{(i)}$ and $d^{(i)}$. Set $d^{(i+1)} = d^{(i)}$.

Step 1   Obtain $h^{(i)}$ by solving (7) with $d = d^{(i+1)}$. Let $d^{i+1} = \left\| h^{(i)} \right\|_2$.

Step 2   Evaluate $x_{em}^{(i+1)}$ using (5) and set $V = \{x_{em}^{(i+1)}\}$.

Step 3   Apply multi-point parameter extraction using the points in the set V to obtain $f^{(i+1)}$.

Step 4   If the success criteria of (31) and (32) are satisfied update the matrix $B^{(i)}$ to $B^{(i+1)}$ using Broyden's formula [8] and update d Go to Step 10.

Comment   The trust region size d is updated based on how the predicted reduction in $\left\| f \right\|_2$ agrees with the actual reduction.

Step 5   If the success criterion of (32) is not satisfied obtain $J_{os}^{(i)}$ and from which evaluate $J_{em}^{(i)} = J_{os}^{(i)} B^{(i)}$. Switch to the second phase. Go to Step 10

Comment The second phase takes as arguments $x_{em}^{(i)}$ and $J_{em}^{(i)}$ and returns $x_{em}^{(k)}, B^{(k)}$ and $f^{(k)}$. It should

be clear that several iterations might be executed in the second phase before switching back to

phase 1.

Step 6 If $|V|$ is equal to one go to Step 9.

Comment $|V|$ denotes the cardinality of the set *V*.

Step 7 Compare $f^{(i+1)}$ obtained using $|V|$ fine model points with that previously obtained using $|V|-1$

fine model points. If $f^{(i+1)}$ is approaching a limiting value update the matrix $B^{(i)}$ to get $B^{(i+1)}$,

obtain $J_{os}^{(i+1)}$, evaluate $J_{em}^{(i+1)} = J_{os}^{(i+1)} B^{(i+1)}$ and switch to phase 2. Go to Step 10.

Step 8 If $|V|$ is equal to *n*, obtain the matrix $J_{em}^{(i+1)}$ using the fine model points in the set *V*. Switch to

phase 2. Go to step 10.

Step 9 Obtain a temporary point using $x_{em}^{(i+1)}, f^{(i+1)}$ and $d^{(i+1)}$. Add this point to the set *V* and go to

Step 3.

Step 10 Let *i=i+1*. Go to Step 0.

The second phase can be summarized in the following steps

Phase 2

Step 0 Given the current iterate of the space mapping technique $x_{em}^{(i)}$ and the corresponding fine model

responses Jacobian matrix $J_{em}^{(i)}$.

Step 1 Obtain a successful iterate $x_{em}^{(k)}$ by solving

$$(J_{em}^{(i)T} J_{em}^{(i)} + lI)\Delta x = -J_{em}^{(i)T} g .$$

For a suitable value of l that satisfies the success criterion for the objective function (32).

Step 2 Apply parameter extraction at this point to get $f^{(k)}$.

Comment Multi-point parameter extraction is used at this step to ensure the uniqueness of the extracted

parameters.

Step 3   If the success criterion of (31) is satisfied obtain $\boldsymbol{J}_{os}^{(k)}$ at the point $\boldsymbol{x}_{os}^{(k)} = \boldsymbol{P}(\boldsymbol{x}_{em}^{(k)})$, evaluate the

matrix $\boldsymbol{B} = \left(\boldsymbol{J}_{os}^{(k)T} \boldsymbol{J}_{os}^{(k)} \right)^{-1} \boldsymbol{J}_{os}^{(k)T} \boldsymbol{J}_{em}^{(k)}$ and switch to phase 1.

Step 4   If the termination condition is satisfied invoke the minimax optimizer else go to Step 1.

The solution obtained from this algorithm is the optimal fine model design. Also, the technique still generates the information about the mapping between the two spaces presented by the matrix $\boldsymbol{B}$. A flowchart for the first phase of the proposed algorithm is shown in Fig. 9.

VI. EXAMPLES

An HTS Filter.

A Balanced Microstrip Filter.

VII. CONCLUSIONS

In this paper we presented a hybrid algorithm of space mapping. This algorithm enables smooth switching from space mapping to direct optimization if space mapping fails. It utilizes all the available information accumulated by space mapping in direct optimization. The algorithm also enables smooth switching from direct optimization to space mapping if space mapping is converging smoothly. The connection between space mapping and direct optimization is based on a novel theory that was presented. A number of examples were solved using the suggested algorithm and the results are encouraging.

REFERENCES

[1]   J.W. Bandler, R.M. Biernacki, S.H. Chen, P.A. Grobelny and R.H. Hemmers, "Space mapping technique for electromagnetic optimiztion," *IEEE Trans. Microwave Theory Tech.,* vol. 42, 1994, pp. 2536-2544.

[2]   J.W. Bandler, R.M. Biernacki, S.H. Chen, R.H. Hemmers and K. Madsen, "Electromagnetic optimization exploiting aggressive space mapping," *IEEE Trans. Microwave Theory Tech.*, vol. 43, 1995, pp. 2874-2882.

[3]   J.W. Bandler, R.M. Biernacki and S.H. Chen, "Fully automated space mapping optimization of 3D structures," *IEEE MTT-S Int. Microwave Symp. Dig.* (San Francisco, CA), 1996, pp. 753-756.

[4]   M.H. Bakr, J.W. Bandler, R.M. Biernacki, S.H. Chen and K. Madsen, " A trust region aggressive space mapping algorithm for EM optimization," *IEEE MTT-S Int. Microwave Symp. Dig.* (Baltimore, MD.), 1998, pp. 1759-1762.

[5]   J.J. Moré and D.C. Sorenson, "Computing a trust region step," *SIAM J. Sci. Stat. Comp.*, vol. 4, 1983, pp. 553-572.

[6]   C.G. Broyden, "A class of methods for solving nonlinear simultaneous equations," *Math. Comp.*, vol. 19, 1965, pp. 577-593.

[7]   R. Fletcher, Practical Methods of Optimization, Second Edition, John Wiley & Sons Ltd., 1987.

[8]   J.W. Bandler, W. Kellermann and K. Madsen, "A superlinearly convergent minimax algorithm for microwave circuit design," *IEEE Trans. Microwave Theory Tech.*, vol. MTT-33, 1985, pp. 1519-1530.
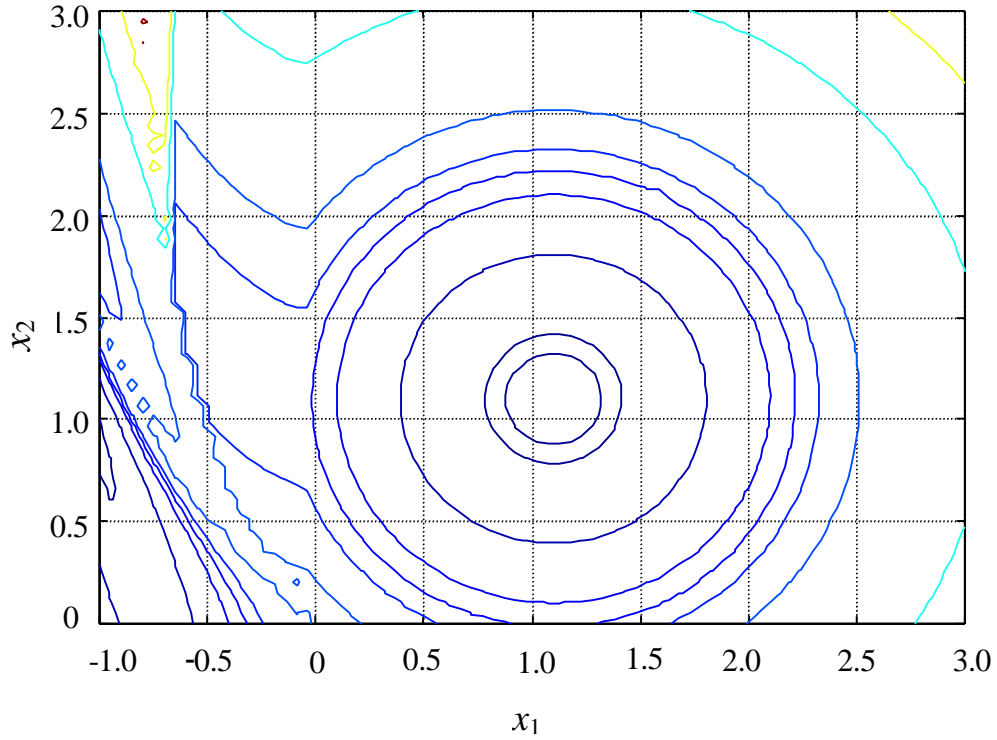
Fig. 1. The contours of the function $\|\boldsymbol{f}\|_2$ for the case $\boldsymbol{a}_1 = -0.1$ and $\boldsymbol{a}_2 = -0.1$.
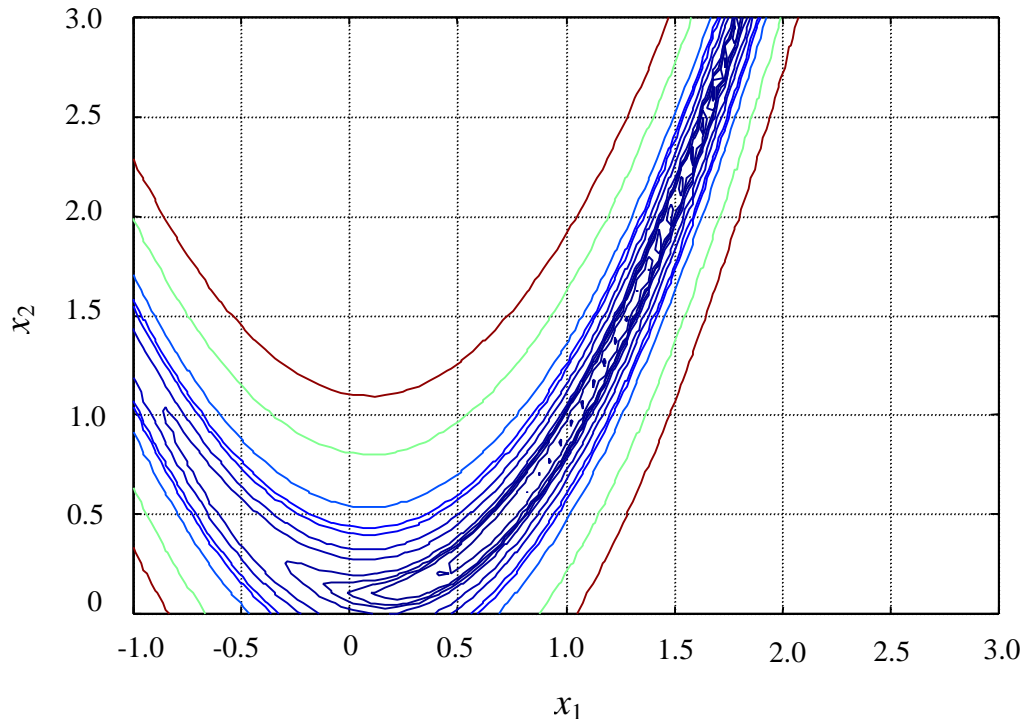
Fig. 2. The contours of the Rosenbrock function for the case $\boldsymbol{a}_1 = -0.1$ and $\boldsymbol{a}_2 = -0.1$.
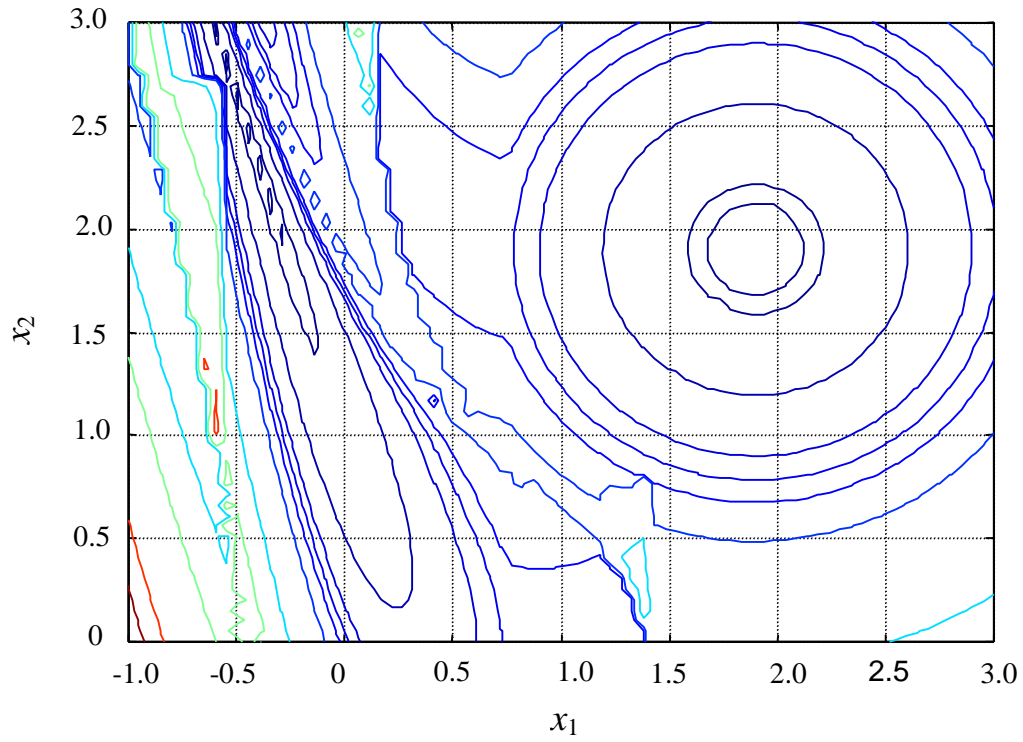
Fig. 3. The contours of the function $\|\boldsymbol{f}\|$, for the case $\boldsymbol{a}_1 = -0.9$ and $\boldsymbol{a}_2 = -0.9$.
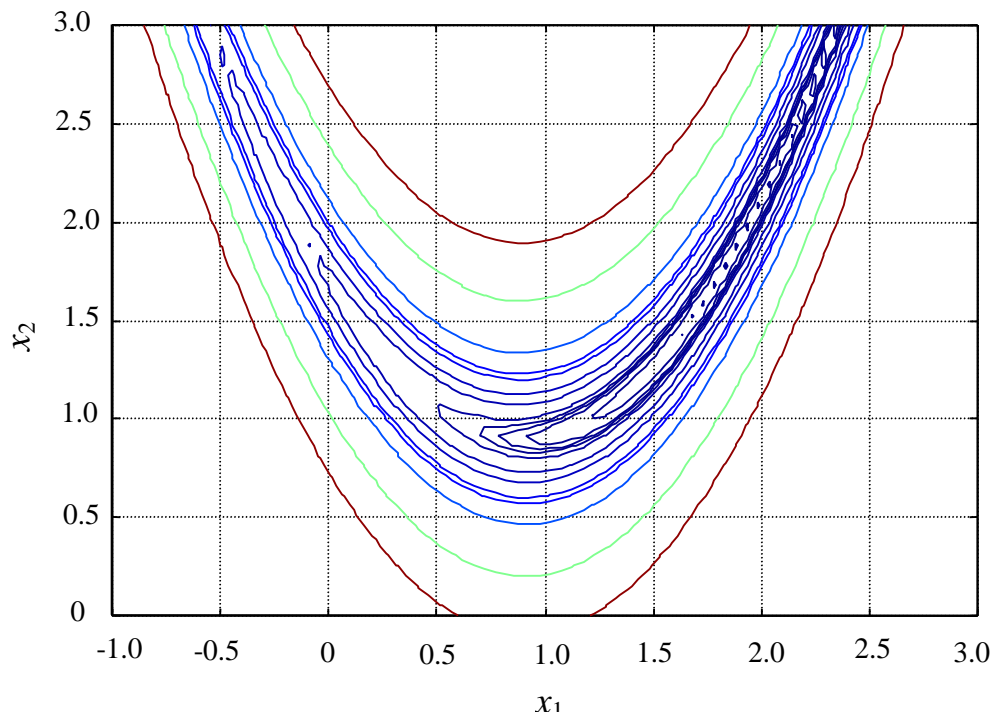
Fig. 4. The contours of the Rosenbrock function for the case $\boldsymbol{a}_1 = -0.9$ and $\boldsymbol{a}_2 = -0.9$.

19
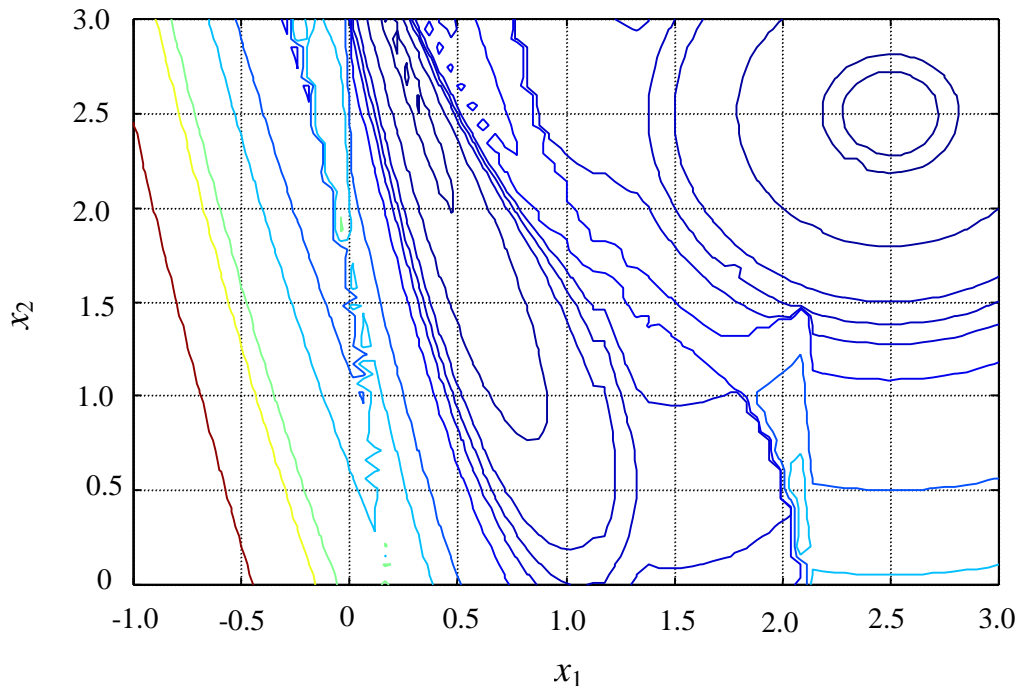
Fig. 5. The contours of the function $\|f\|_2$ for the case $a_1 = -1.5$ and $a_2 = -1.5$.
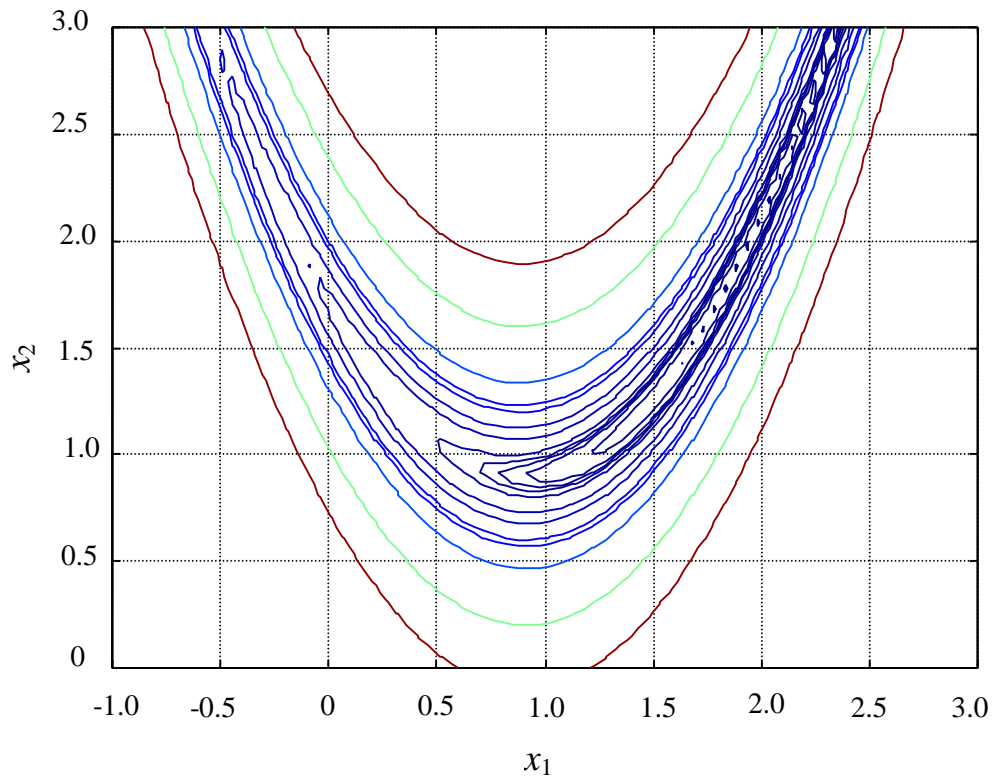
Fig. 6. The contours of the Rosenbrock function for the case $a_1 = -1.5$ and $a_2 = -1.5$.

20

$$J_{em} = J_{os}B$$
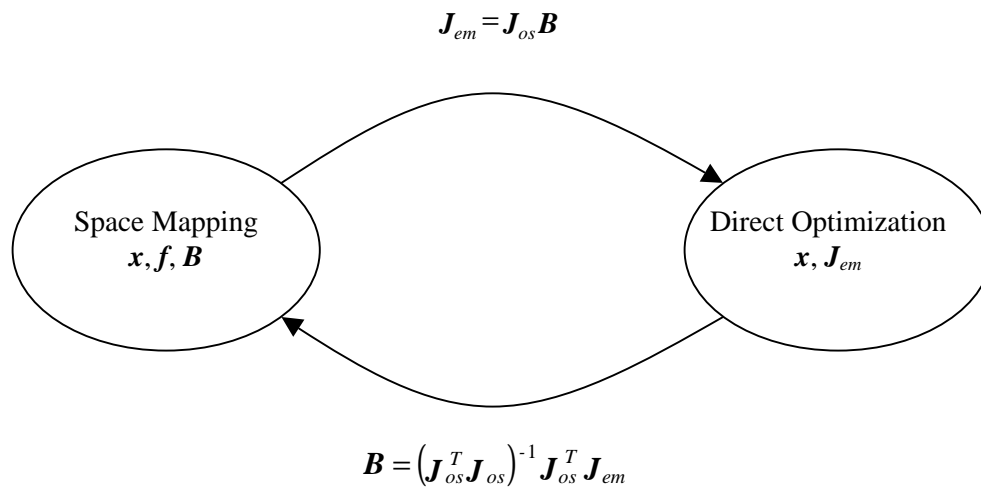
Fig. 7. Illustration of the connection between space mapping and direct optimization.

$$B = \left(J_{os}^{T} J_{os} \right)^{-1} J_{os}^{T} J_{em}$$
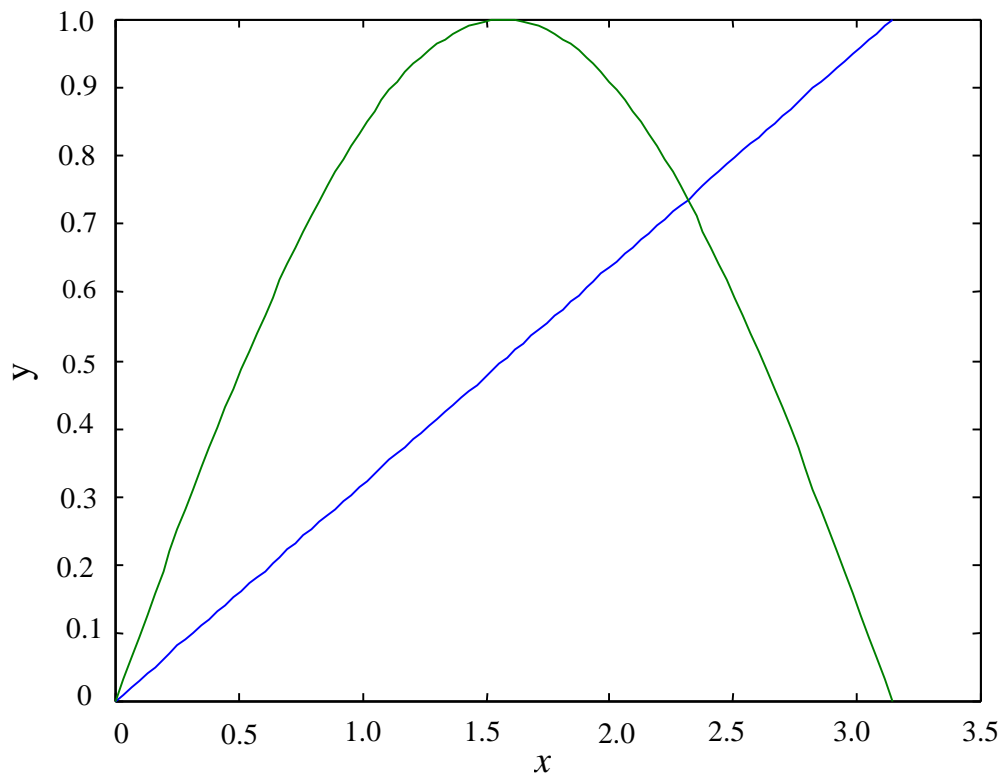
Fig. 8. The coarse and fine model responses for the first illustration of theorem I
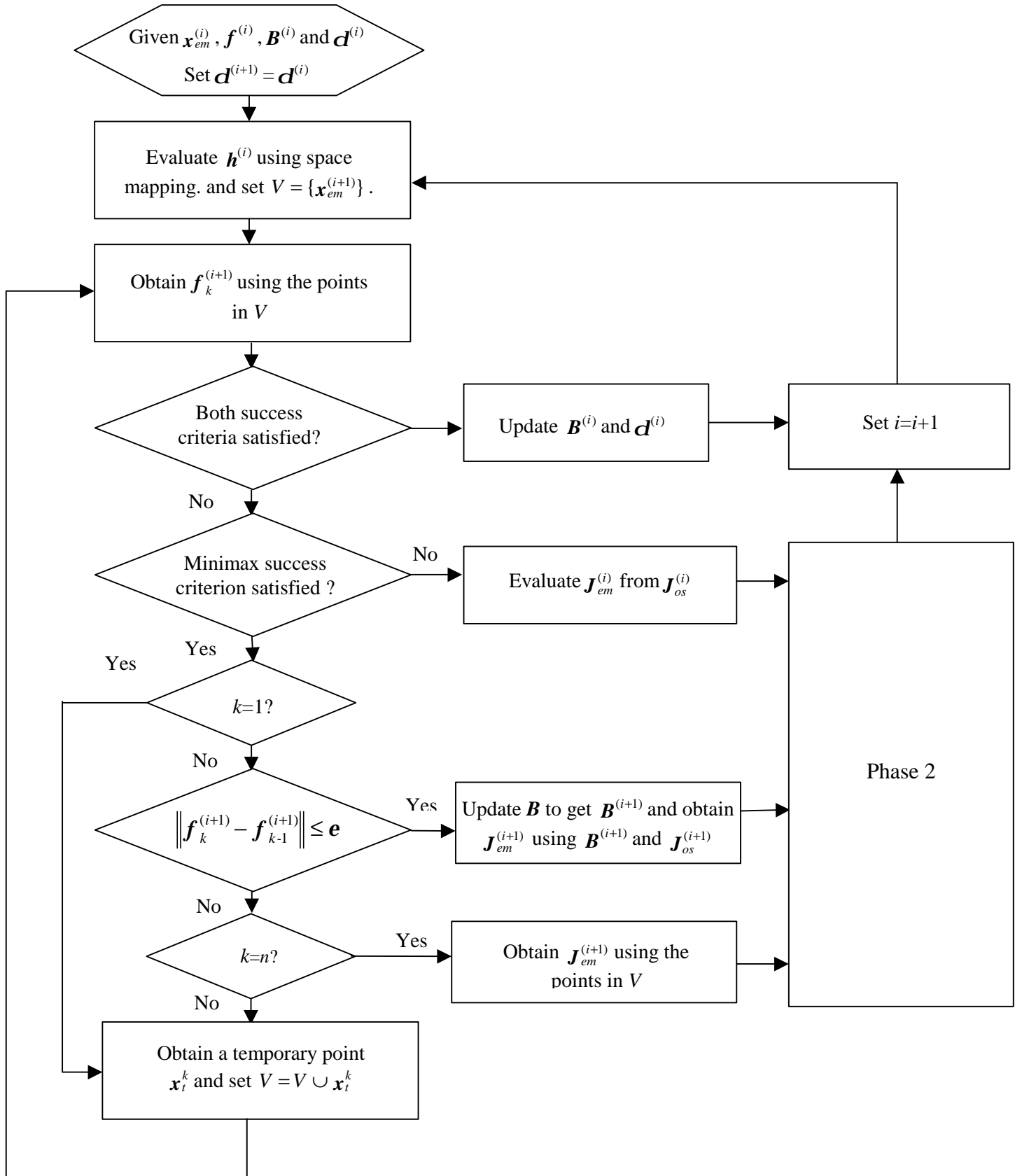
Fig. 9. A flow chart of the first phase of the proposed algorithm.